Influence of Ball-milling on Sintered Body Density of Fine Tungsten Powder

Influence of Ball-milling on Sintered Body Density of Fine Tungsten Powder

Lingjie Duan[1,*], Jinglian Fan[2]

[1]School of Materials Science & Engineering, Tianjin University, Tianjin, China
[2]State Key Laboratory for Powder Metallurgy, Central South University, Changsha, China

*Corresponding author e-mail: dlj14141144@hotmail.com

Abstract. The fine pure tungsten powder with a BET particle size of 0.14 μm was prepared by sol spray drying-calcination-hydrogen reduction process. The influences of ball-milling ways (dry-milling and wet-milling) on the tungsten powder morphology and powder formability were investigated. The changes of pure tungsten properties with sample size (small samples with a thickness of 2.5mm and big samples with a thickness of 2cm) were explored. In addition, the variation of microstructure and grain size with different ball milling way and sample size was studied in detail. Results show that both dry-milling and wet-milling have a great improvement in powder formability. The densities of dry-milling sintered bodies are obviously higher than that of wet-milling bodies. At the same time, the density distribution of dry-milling sintered bodies is more uniform in big samples. The wet-milling powder has a wider particle size distribution and a strong activation effect, thus the wet-milling powder sintered body has a coarser grain.

1. Introduction

Tungsten has the advantages of high melting point, high density, high strength, high hardness, high wear resistance, low thermal expansion coefficient, good corrosion resistance and antioxidant properties, which make tungsten materials widely used in aerospace, national defense and civil industry, such as the counterweight, shock absorbing material and plasma facing materials [1-3]. With the development of tungsten in the high point field, the requirements of its density, physical properties and size are almost strict [4, 5]. However, due to the high melting point of tungsten (above 3410℃), the sintering performance of tungsten is very poor, especially for some large samples. There are mainly several solutions to this problem:

(I)Fine-grained and nanocrystalline powders, (II)Spark Plasma Sintering (SPS), hot pressing, hot isostatic pressing (HIP) and other special processing technology and (III)High energy ball milling and addition of forming agent.

However, the study of different ball-milling ways and sizes is inadequate. This paper mainly studies the reasonable process of sintering ultrafine grained pure tungsten samples with different sizes by adjusting the ball-milling ways.

2. Experimental description

2.1 Preparation of powder

Ammonium polytungstate $(NH_4)_6H_2W_{12}O_{40}\cdot 5H_2O$ and a small quantity of polyethylene glycol (PEG) were mixed with acid and alkali reagents to form a solution colloid. The precursor powder of tungsten oxide was obtained by spray drying. Then after calcining for 2h at 400℃, grinding and sieving, the powder was reduced for 2h at 550℃ and 3h at 790℃. The ultrafine tungsten powder (62.5nm) was obtained.

Because the reduced powder is hard to form, the ultrafine tungsten powder obtained by the reduction was activated on the planetary ball mill, and two different ball-milling methods were used to activate the pure tungsten powder. In wet milling, the ball-to-powder weight ratio is 2:1, the solid-to-liquid volume ratio is 1:2, the ball-milling time is 10 h, and the rotating speed is 198r/min. In dry milling, the ball-to-powder weight ratio is 1:3, ball-milling time is 3h, and the rotating speed is 113r/min. The ball-milling jar is stainless steel, the grinding ball is tungsten ball, and the jar is protected by high purity Ar gas.

XRD analysis of different powders was carried out. The grain sizes of the powders were estimated by X-ray diffraction spectrum and Williamson-Hall equation. The Williamson-Hall equation can be written as:

$$\beta \cos\theta = 0.9(\lambda/\mathrm{d}) + 2\varepsilon \sin\theta, \quad (1)$$

where β is the half width of diffraction peak, θ is Bragg angle, λ is X-ray wavelength, d is grain size, and ε is internal stress.

The specific surface areas of the powders were analyzed. The specific surface areas of the powders were evaluated by the following formula:

$$d_{BET} = 6/(S_{BET}\rho_t), \quad (2)$$

where d_{BET} is the calculated particle size, S_{BET} is the specific surface area of the powder, and ρ_t is the theoretical density of the powder, which is 19.3 g/cm^3.

SEM analysis of different powders was carried out to observe the size and morphology of the powders. The particle size distribution of different powders was analyzed by laser particle size detection.

2.2 Forming and sintering

Different ultra-fine tungsten powders (reduced powder, wet-milling powder and dry-milling powder) were used to form small samples with a thickness of 2.5mm and big samples with a thickness of 2cm. The large samples and small samples were put into tungsten-rod furnace and sintered for 2h at 2000℃. The heating rate was 2℃/min. The small sample sintered from dry-milling powder is represented by

DS, the big sample sintered from dry-milling powder is represented by DB, the small sample sintered from wet-milling powder is denoted by WS, and the big sample sintered from wet-milling powder is denoted by WB.

The density and density distribution of sintered bodies with different preparation methods were determined by Archimedes drainage method. The tensile fractures of sintered bodies with different preparation methods were analyzed by SEM, and the grain size, fracture type and density were analyzed.

3. Results

3.1 The grain size and particle size

Fig. 1 is the XRD diagram of the three kinds of powders. In Table 1, the characteristic parameters for the three types of powders obtained from the testings and formula calculation are listed. It can be seen from Fig. 1 that the X ray diffraction peak is thinning during dry milling, while wet milling makes the peak broaden. This is due to the grain refinement by wet milling. Because of the higher temperature, the grain grow up during the process of welding in dry milling. It can be seen from Table 1 that dry milling has reduced the particle size of BET, while wet milling has increased BET particle size. This is because the agglomerations in the reduced powder is broken through the dry milling, and the particle size of BET is reduced. The wet milling process has a long milling time, so there was a thin slice of aggregation after the breakage. Therefore, the particle size of the BET becomes larger.

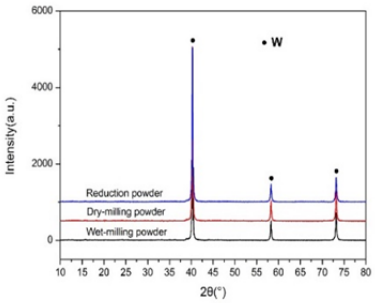

Figure 1. XRD patterns of the three types of powders

Table 1. Characteristic parameters for three types of powders

powder	Grain size/nm	specific surface area/$m^2 \cdot g^{-1}$	d_{BET}/μm
Reduced	62.5	2.23	0.14
Dry-milling	66.2	2.72	0.11
Wet-milling	57.7	1.83	0.17

Fig. 2 is the SEM images for three kinds of powders, (a), (c) and (e) are the 1200 times morphologies, (b), (d) and (f) are the 40000 times morphologies. In the 1200 times morphologies, there are many large spherical shell aggregates in the reduced powder, and the two ball milling ways both break the agglomeration. In the 40000 times morphologies, the thin slice of aggregations in the wet-milling powder can be found. These are consistent with the information obtained in Fig. 1 and Table 1.

Fig. 3 shows the laser particle size detection results for three kinds of powder. A large number of agglomerations with big particle sizes can be seen from Fig. 3(a) and also be found in Fig. 2 (a). In dry milling and wet milling, the big agglomerations disappear. The particle size distribution of dry-milling powder is relatively concentrated, while the particle size distribution of wet-milling powder is wider.

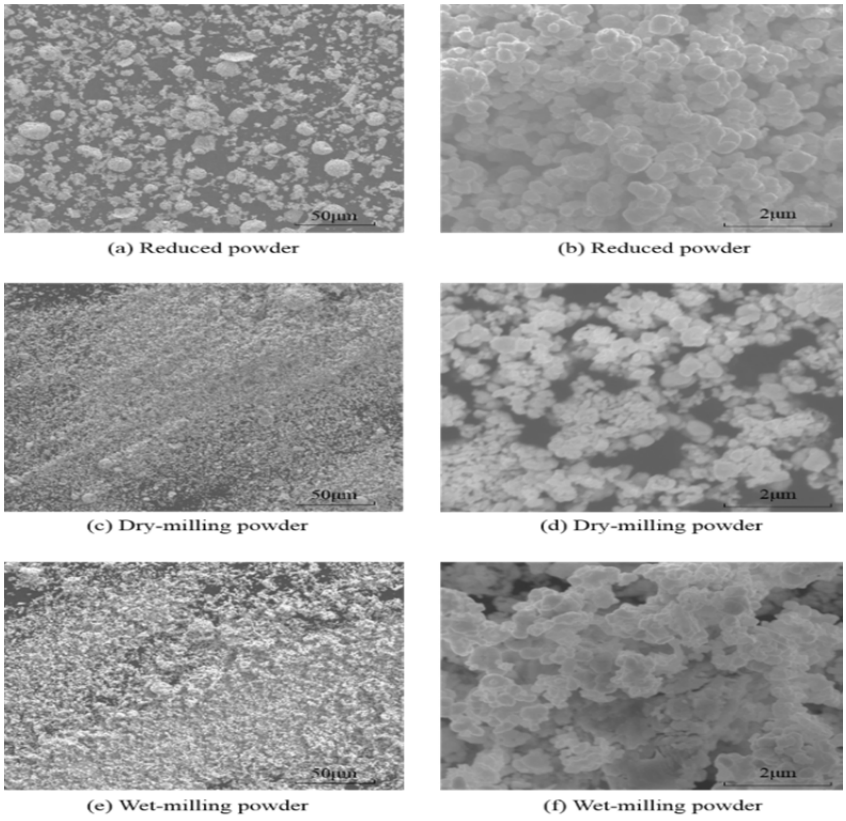

Figure 2. SEM morphologies for three kinds of powders

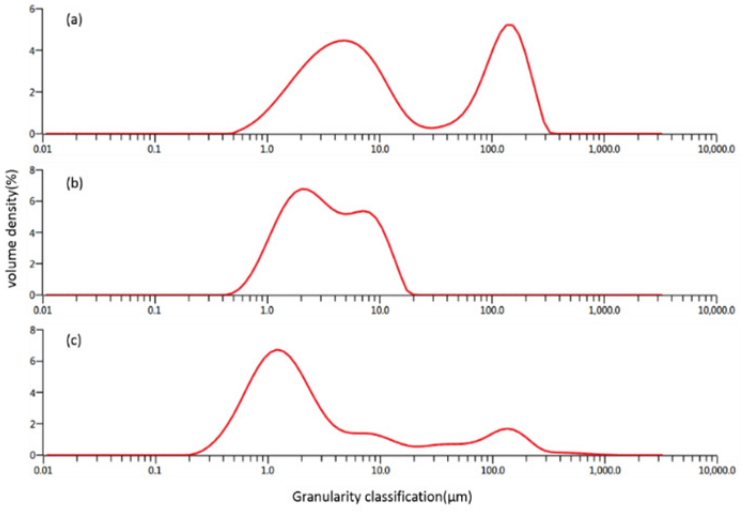

Figure 3. Particle size distribution diagram for three kinds of powders: (a) reduced powder; (b) dry-milling powder; (c) wet-milling powder

3.2 Density

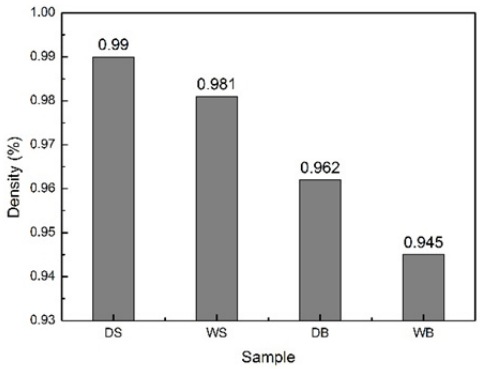

Figure 4. The densities of small and big samples sintered by different powders

Fig. 4 is the density of four different samples. It can be found that the density of wet-milling sintered samples is lower than that of dry-milling sintered samples, and it is more obvious in large samples. This is due to the high activity of wet-milling powder and the wider distribution of particle size. Thus it is easy to form a closed pore by the growth of grain in the early stage of sintering and obstruct the densification process at the later stage of sintering. In large samples, because the sample itself is larger, it is easier to form a closed hole. Therefore, in big samples, the density difference caused by different ball milling ways is more obvious. The density of the small samples is higher than that of the big samples. Because the internal heating is relatively insufficient for big simples, and easy to form closed pores, so the density is smaller than that of small samples.

Table 2. The density and the density variance of big sample sintered by different powders

Property	DB	WB
Density/%	0.962	0.945
Density variance/%^{2}	$1.29*10^{-5}$	$1.25*10^{-4}$

Table 2 is the density and density variance of big samples. Because the thickness of the big samples is larger (2cm), the density distribution is obviously uneven. The density in our data is the average density. However, in the actual use of samples and later deformation processing, whether the density distribution is uniform is very important. The density variance is used to comparative analysis here. It can be found that the density distribution of DB is more uniform than that of WB, and its density variance is 10 times smaller than that of WB. It is further illustrated that the wet-milling powder has high activity, easily produces closed pore, reduces density and makes the inhomogeneity of density distribution.

3.3 Fracture morphology of sintered body

Fig. 5 shows tensile fracture SEM pictures of samples prepared by different preparation methods. It can be seen that the grain size of the small sample is slightly larger than that of the large sample. This is due to the fact that the smaller samples are more fully heated.

In addition, as the dry-milling time is short and the rotational speed is low, the activation effect is not as good as the wet-milling powder. According to Fig. 3, it can be seen that the particle size distribution for wet-milling powder is more extensive, and the curvature difference between particles provides a great driving force on grain growth during the later stage of sintering, which makes the grain easier to grow [6]. Therefore, the grains of the dry-milling powder sintered body are finer, while the grains in wet-milling powder grow obviously.

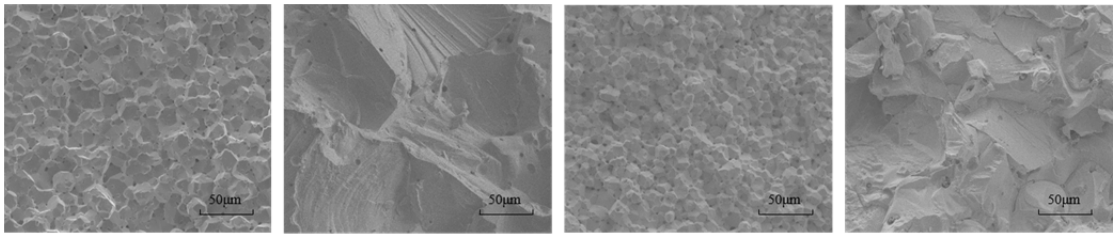

Figure 5. Fracture SEM morphologies of the four kinds of samples

4. Conclusions

(a) Both dry milling and wet milling can effectively improve the formability of the powder by crushing the agglomeration and activation of ball milling.

(b) Because the grain of sintered body prepared by wet milling is easy to grow and promote the production of closed pore, its density is lower than that of dry milling, and its density distribution in large samples is more uneven than that of powder prepared by dry milling way.

(c) The particle size distribution of wet-milling powder is wider, which provides driving force for grain growth. Moreover, because of the short milling time and low rotational speed, the dry-milling powder has less activation effect than wet-milling powder . So the grain of dry powder sintered body is finer.

Acknowledgments

This work was financially supported by the NNSF of China (No. 51534009).

References

[1] B. Huang, J. Fan, Research and application of nano tungsten material, China Tungsten Industry, 2001, 16(5/6): 38-44.

[2] J. Fan, B. Huang, D. Wang, et al. Preparation technology of nanometer size refractory high density tungsten based alloy composite powders, Rare Metal Materials & Engineering, 2001, 30(6):404-405.

[3] S.J. Zinkle, M. Victoria, K. Abe, Scientific and engineering advances from fusion materials R&D, Journal of Nuclear Materials, 2002, 307(Part 1):31-42.

[4] B.D. Wirth, K.D. Hammond, S.I. Krasheninnikov, Challenges and opportunities of modeling plasma–surface interactions in tungsten using high-performance computing, Journal of Nuclear Materials, 2015, 463:30-38.

[5] N. Lemahieu, M. Balden, S. Elgeti, H/He irradiation on tungsten exposed to ELM-like thermal shocks, Fusion Engineering & Design, 2016, 109–111(Part A):169-174.
[6] R.M. German, Sintering Theory and Practice, New York: John Wiley & Sons, 1996.